GNAT versus POD-DEIM for Model Order Reduction of Electrical Networks with Semiconductors

Michael Hinze and Ulrich Matthes

[1] Michael Hinze, Department of Mathematics, University of Hamburg, Bundesstr. 55, 20146 Hamburg, Germany,
michael.hinze@uni-hamburg.de
[2] Ulrich Matthes, Department of Mathematics, University of Hamburg, Bundesstr. 55, 20146 Hamburg, Germany,
ulrich.matthes@math.uni-hamburg.de

Abstract. In this paper we consider model order reduction (MOR) techniques for electrical networks with semiconductors modeled by the drift-diffusion equations. We compare the Gauß-Newton with approximated tensors (GNAT) MOR method with the POD-DEIM approach.

Keywords: Model Order Reduction, Parametrized Dynamical Systems, Drift-Diffusion Equations, Integrated Circuits, GNAT, POD-DEIM

AMS subject classifications: 93A30, 65B99, 65M60, 65M20

1 Introduction

Electrical networks with complex components like semiconductors can be reduced using MOR methods. Here we compare the proper orthogonal decomposition (POD) approach with the discrete empirical interpolation method (DEIM) for the reduction of the nonlinearities, see e.g. [8], with the Gauß-Newton with approximated tensors (GNAT) method, see [4]. We emphasize that our MOR approach is not restricted to electrical networks with semiconductors but also extends to networks containing many simple components, and complex components modeled by PDE systems (see Figure 1) if the network allows modeling with modified nodal analysis (MNA), see e.g. [9]. In a companion paper [11] we compare the MOR of semiconductors in electrical networks modeled by drift-diffusion (DD) and quantum-drift-diffusion (QDD)-equations and present numerical results obtained by a simple interpolation method.

This paper is organized as follows. In Section 2 we describe the mathematical model for the electrical network with semiconductors. In Section 3 we describe the implementation of the GNAT method. In Section 4 we compare GNAT and POD-DEIM for an example using the nonlinear heat transport equation. In Section 5 we compare GNAT and POD-DEIM and present numerical results for a

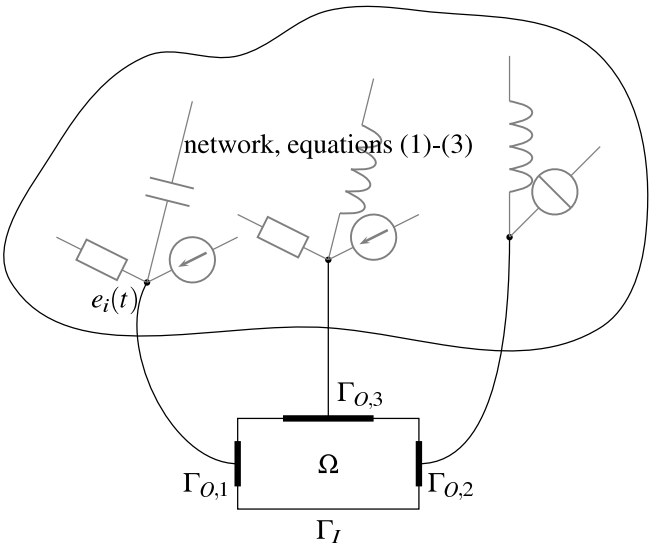

Fig. 1. Sketch of a network with many simple components and a complex component representing a semiconductor.

simple test circuit. We find, that the GNAT method allows for lower approximation errors for the same Ansatz space, the POD-DEIM method is preferable due to its simplicity, and its far better stability properties, especially in the case of MOR for PDE systems.

2 Modeling of the electrical network with semiconductors

We now describe the mathematical model for electrical networks with many simple components like resistors, capacitors, and inductors and complex components like semiconductors modeled by DD equations. First the network containing only the simple components is modeled by a differential algebraic equation (DAE) system which is obtained by a modified nodal analysis (MNA) [12], including the Ohmic contacts $\Gamma_{O,k}, k = 1, \ldots, N_c$ of the semiconductors as network nodes. Denoting by e the node potentials and by j_L, j_V, and j_S the currents of inductive, voltage source, and semiconductor branches, the DAE reads (see, e.g. [7, 12, 14])

$$A_C \frac{d}{dt} q_C(A_C^\top e, t) + A_R g(A_R^\top e, t) + A_L j_L + A_V j_V + A_S j_S = -A_I i_s(t), \quad (2.1)$$

$$\frac{d}{dt} \phi_L(j_L, t) - A_L^\top e = 0, \quad (2.2)$$

$$A_V^\top e = v_s(t). \quad (2.3)$$

Here, the incidence matrix $A = [A_R, A_C, A_L, A_V, A_S, A_I] = (a_{ij})$ represents the network topology, e.g. at each non mass node i, $a_{ij} = 1$ if the branch j leaves

node i and $a_{ij} = -1$ if the branch j enters node i, and $a_{ij} = 0$ else. The indices R, C, L, V, S, I denote the capacitive, resistive, inductive, voltage source, semiconductor, and current source branches, respectively. In particular the matrix A_S denotes the semiconductor incidence matrix. The vector valued functions q_C, g and ϕ_L are continuously differentiable defining the voltage-current relations of the network components. The continuous vector valued functions v_s and i_s are the voltage and current sources. For details we refer to [9].

In a second step the semiconductors are modeled by PDE systems, which are then coupled to the DAE of the network via the nodes related to the Ohmic contacts. Here we first use the transient drift-diffusion equations as a continuous model for semiconductors, see e.g. [1, 2] and the references cited there. Using the notation and scaling introduced there, we obtain the following scaled system of PDEs for the electrostatic potential $\psi(t,x)$, the electron and hole concentrations $n(t,x)$ and $p(t,x)$ and the current densities $J_n(t,x)$ and $J_p(t,x)$:

$$\lambda \Delta \psi = n - p - C, \tag{2.4}$$

$$-\partial_t n + \nu_n \operatorname{div} J_n = \quad R(n,p), \tag{2.5}$$

$$\partial_t p + \nu_p \operatorname{div} J_p = -R(n,p), \tag{2.6}$$

$$J_n = \quad \nabla n - n \nabla \psi, \tag{2.7}$$

$$J_p = -\nabla p - p \nabla \psi. \tag{2.8}$$

Here $(t,x) \in [0,T] \times \Omega$ and $\Omega \subset \mathbb{R}^d, d = 1,2,3$. The nonlinear function R describes the rate of electron/hole recombination, where we focus on the Shockley-Read-Hall recombination

$$R(n,p) := \frac{np - n_i^2}{\tau_p(n + n_i) + \tau_n(p + n_i)}$$

which does not depend on the current densities. Here, τ_n and τ_p are the average lifetimes of electrons and holes, and n_i is the constant intrinsic concentration which satisfies $n_i^2 = np$ if the semiconductor is in thermal equilibrium. The scalar $\lambda > 0$ is the scaled Debye length, and ν_n and ν_p are the scaled mobilities of electrons and holes. The temperature is assumed to be constant which leads to a constant thermal voltage U_T. The function C is the time independent doping profile.

This system is supplemented with the boundary conditions

$$\psi(t,x) = \psi_{bi}(x) + (A_S^\top e(t))_k = U_T \log\left(\frac{\sqrt{C(x)^2 + 4n_i^2} + C(x)}{2n_i}\right) + (A_S^\top e(t))_k, \tag{2.9}$$

$$n(t,x) = \frac{1}{2}\left(\sqrt{C(x)^2 + 4n_i^2} + C(x)\right), \quad p(t,x) = \frac{1}{2}\left(\sqrt{C(x)^2 + 4n_i^2} - C(x)\right), \tag{2.10}$$

for $(t,x) \in [0,T] \times \Gamma_{O,k}$, where the potential of the nodes which are connected to a semiconductor interface enter in the boundary conditions for ψ. Here, $\psi_{bi}(x)$ denotes the build-in potential and n_i the constant intrinsic concentration. All other

parts of the boundary are isolation boundaries $\Gamma_I := \Gamma \setminus \Gamma_O$, where $\nabla\psi \cdot \nu = 0$, $J_n \cdot \nu = 0$ and $J_p \cdot \nu = 0$ holds. The semiconductor model (2.4)-(2.8) is coupled to the network through the semiconductor current vector j_S with the components

$$j_{S,k} = \int_{\Gamma_{O,k}} (J_n + J_p - \varepsilon\partial_t\nabla\psi) \cdot \nu \, d\sigma, \; k = 1, \ldots, N_c, \tag{2.11}$$

where ν denotes the unit outward normal to the interface $\Gamma_{O,k}$. Further details are given in [9]. Contributions to the analytical and numerical analysis of PDAE systems of the presented form can be found in [2, 6, 13, 14].

3 Gauß-Newton with Approximated Tensors (GNAT)

In this section we describe our implementation of the GNAT method. Numerical results comparing GNAT with POD-DEIM are given in Section 5.

The GNAT method is a nonlinear MOR method, which is introduced in [3] for MOR of fluid-dynamic applications.

Let us describe the GNAT approach for a time-dependent PDE system which already is semi-discretized with respect to the spatial variable be, e.g. the finite element method or the finite volume approach. Then we are left with a nonlinear ODE-system of the from

$$\dot{y}(t) = F(y(t), t; \mu) \qquad y(0) = y_0(\mu),$$

where μ is some parameter. Implicit time integration then yields a sequence of nonlinear problems which at time instance t_n are of the form

$$R^n(y^{n+1}; \mu) = 0,$$

i.e. at every time step we have to solve a nonlinear residual equation of the form

$$R(y) = 0.$$

For its solution we consider the Ansatz

$$y = y^{(0)} + \Phi_y y_r,$$

where $y^{(0)}$ is some given reference vector and Φ_y is the POD basis obtained from the snapshots computed at the given time instances. Since the dimension n_y of y_r in general is much smaller than the dimension n_0 of $R(y)$ we are left with the nonlinear least squares problem

$$\min_{y \in y^{(0)} + <\Phi_y>} \|R(y)\|_2, \quad (T2)$$

which we solve with the Gauss-Newton method; $k = 0, y_r^{(0)}$ given

$$p^{(k)} = \arg\min_{a \in R^{n_y}} \|J^{(k)}\Phi_y a + R^{(k)}\|_2,$$

$$y_r^{(k+1)} = y_r^{(k)} + \alpha^{(k)} p^{(k)}, \quad k = k+1.$$

Here, $J^{(k)}$ denotes the Jacobian of R at $y_r^{(k)}$ and $\alpha^{(k)} > 0$ the size of the Gauss-Newton step. The solution of this least squares problem is at least as expensive as the solution of the full model, because it involves a large, dense $n_0 \times n_y$ matrix, instead of a usually large, but sparse n_0^2 problem, and some Gauss-Newton iterations. Only the ansatz space for the variables y is reduced. To reduce the computational complexity we solve the least-squares problem only approximately, through approximating $R^{(k)}$ and $J^{(k)}\Phi_y$ by some appropriate low rank approximations. These low-rank approximations are obtained through the selection of appropriate rows similar to the DEIM approach. Let $\hat{\cdot}$ denote the restriction operator to the sample indices, and Φ_R, Φ_J POD-bases of snapshots from $R^{(k)}$ and $J^{(k)}\Phi_y$, respectively. We set

$$R^{(k)} \approx \Phi_R R_r^{(k)} \qquad J^{(k)}\Phi_y \approx \Phi_J J_r^{(k)}$$

with

$$R_r^{(k)} = \underset{z \in \mathbb{R}^{n_R}}{\arg\min} \|\hat{R}^{(k)} - \hat{\Phi_R} z\|_2$$

and

$$J_r^{(k)} = \underset{z \in \mathbb{R}^{n_J \times n_y}}{\arg\min} \|J^{\hat{(k)}}\Phi_y - \hat{\Phi_J} z\|_2.$$

In this procedure the selection of the most important indices is done component wise. We take snapshots from (T2), perform a SVD to get the reduced POD-bases Φ_R, Φ_J and apply DEIM to select the most important indices. We note that the number of indices must be at least of the size of the POD basis Φ_y, but to obtain an accurate result a larger number of indices is necessary. This is different from the POD-DEIM approach, where only the nonlinear part is reduced in this way.

We finally obtain the procedure

$$p^{(k)} = \underset{a \in R^{n_y}}{\arg\min} \|\hat{\Phi_J}^{+} J^{\hat{(k)}}\Phi_y a + \Phi_J^T \Phi_R \hat{\Phi_R}^{+} \hat{R}^{(k)}\|_2 \qquad (T3)$$

$$y_r^{(k+1)} = y_r^{(k)} + \alpha^{(k)} p^{(k)},$$

where $\cdot^+$ denotes the pseudo (left)-inverse.

4 Test Example

In this section we use the GNAT method to obtain a reduced order model for the nonlinear heat conduction equation

$$\dot{y} - a\Delta y + by^3 = 0 \text{ in } \Omega \times (0,T),\ y(0) = y_0,\ \partial_\eta y = 0 \text{ on } \partial\Omega \times (0,T), T > 0$$

in the domain $\Omega = (0,1)$. For the parameters we choose $a = 1$ and $b = 1$.

To test the GNAT approach we use the different initial conditions $y_0(x) := \max(0, 1 - |x - 1/2|/h)$ with $h = 1/500$ denoting the discretization parameter, $y_0(x) := x(1-x)$, and $y_0(x) := \chi([z, 1-z])$ for some $0 < z < 0.5$.

For the numerical discretization we apply the implicit Euler scheme with respect to time and continuous, piecewise linear finite elements in space. The same implicit Euler time-discretization with constant step size is used in the full model and the POD and GNAT reduced order models.

m	POD	GNAT-(T2) L^2	GNAT-(T2) H^{-1}	GNAT-(T3) L^2	GNAT-(T3) H^{-1}
1	2.5431	2.5859	6.1429	2.5863	3.0165
2	1.4750	1.5815	2.1789	1.9465	1.7341
3	0.8458	0.9745	0.7983	1.0792	0.7487
4	0.4659	0.5556	0.3944	0.7154	0.3893
5	0.2477	0.2941	0.2013	0.3236	0.1979
6	0.1279	0.1512	0.1028	0.1784	0.1014
7	0.0644	0.0763	0.0519	0.9743	0.0548
8	0.0316	0.0377	0.0256	0.1221	0.0269
9	0.0151	0.0182	0.0123	0.0373	0.0123
10	0.0071	0.0085	0.0058	0.0353	0.0061
1	3.1122	3.2468	3.1023	3.2468	3.1247
2	2.5975	2.7838	2.5671	2.7842	2.5675
3	2.2933	2.8680	2.9654	3.0028	2.1774
4	1.6844	2.1068	1.3497	2.1243	1.3429
5	1.1871	1.5485	1.1526	1.6895	0.9978
6	0.7795	0.9980	0.6094	1.0006	0.6003
7	0.5105	0.6681	0.4001	0.6719	0.3974
8	0.3278	0.4288	0.2520	0.4253	0.2518
9	0.2096	0.2771	0.1615	0.3060	0.1636
10	0.1326	0.1764	0.1026	0.1767	0.1028

Table 1. GNAT: Absolut errors compared to the output of the full model in the L^2- and the H^{-1}-norm. m denotes the number of POD basis functions. Time discretization with implicit Euler and 4096 time steps (upper block), with trapezoidal rule and 1024 time steps (lower block). We use $y_0(x) = \max(0, 1 - |x - 1/2|/h)$ as initial condition.

To compute the residuals in (T2) and (T3) we use the L^2 norm and also the H^{-1} norm. Compared to POD-DEIM, the GNAT approach with the H^{-1} norm perfroms slightly better, but slightly worse with the L^2 norm. Details can

be found in Table 1, where m denotes the number of POD snapshots and the number of indices chosen for (T3) is $2m + 10$.

We note that in this example we do not observe significant differences in the errors between the POD and POD-DEIM MOR.

5 GNAT vs. POD-DEIM for the test circuit

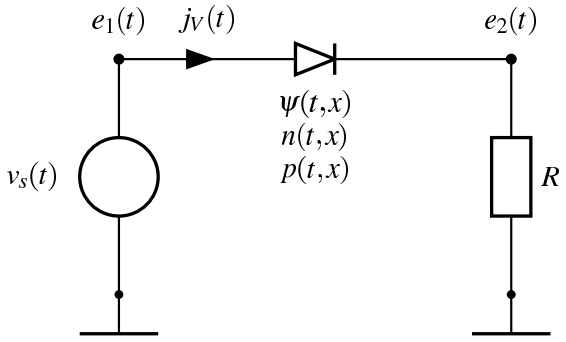

Fig. 2. Basic circuit with one diode.

In this section we compare the GNAT and the POD-DEIM approaches for the circuit in Figure 2. As a time integrator we in both cases use the implicit Euler method.

We start with the simulation of the full model at the frequency $\omega := 10^{10}\ Hz$. The number of POD basis functions s is chosen such that the lack of information content $\Delta(s)$ varies between 10^{-4} to 10^{-8}.

5.1 Numeric results for GNAT and comparison to POD-DEIM

The errors of the reduced models using the GNAT (T2) and (T3) models are given in the Figures 3 and 4.

In Figure 3 (top row), we show the error of the GNAT method with improper scaling and GN initialized with the last time step. The GN method fails in approximately one of 5000 cases, since it converges to a wrong local minimum. But even if this occurs in only one time step, the solution diverges. This can be avoided through initializing the GN iteration with the POD-DEIM solution (lower row). The GN-iteration then converges to the correct minimum in all cases. The GN-iteration improves the POD solution, see Figure 4 (right). The error of the GNAT solution is about a factor two smaller than the error of the POD solution. So using the GNAT as corrector has an additional benefit compared to the POD predictor solution.

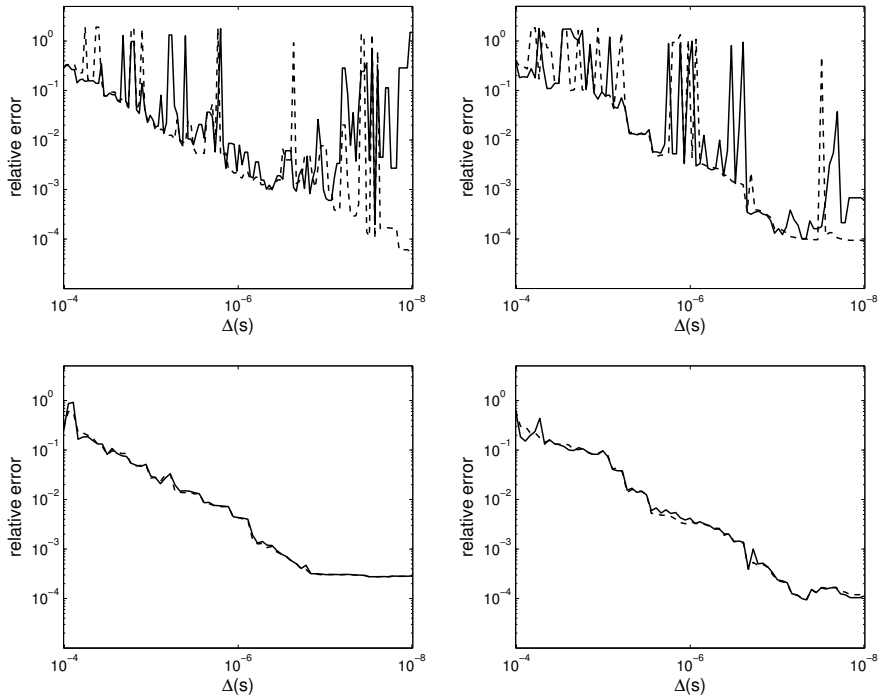

Fig. 3. Error GNAT (T2) (dashed) and GNAT (T3) (solid), 500 FEM ansatz-functions, 200 (left column) and 500 (right column) time steps/snapshots. Upper row: GN iteration initialized with the value at last time step. Lower row: GN iteration initialized with the precalculated POD solution.

There is also the possibility to hand-tune the scaling of the residual blocks to avoid the convergence of the GN-iteration to wrong local minima, see Figure 4 (left), where the results for initialization with the last time step are as good as the results for initialization with the POD solution.

In Figure 5 we compare simulation results for the diode reduced with GNAT, for a bad case, left, from a spike in figure 3, to the correct solution, where the full and GNAT-reduced solution is indistinguishable, right.

5.2 Time Discretization of POD-DEIM and GNAT

In POD-DEIM the reduced system is not discretized in time. Thus an appropriate solver for the DAE system can be chosen, f.e. with automatic order control and time stepping.

The GNAT method on the other hand is time discrete, i.e. it first discretizes in time, and then reduces. So for the control of the time step software packages

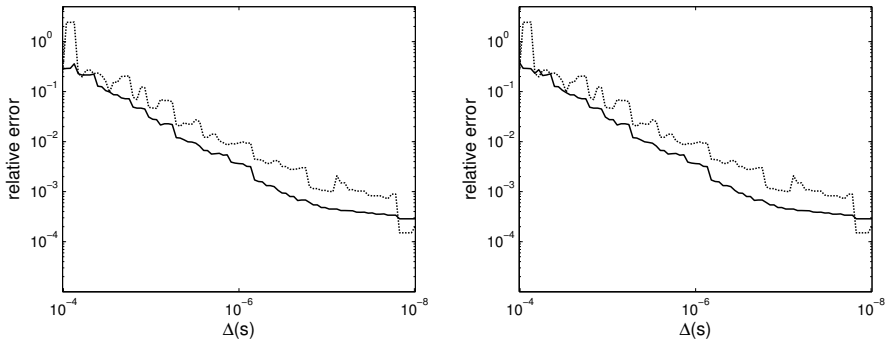

Fig. 4. POD (dots), MOR with GNAT (T3) (solid) with initialization from last time step and hand-tuned scaling of the residual (left). Right: GN starts with POD solution, L^2-Norm of the weighted equations.

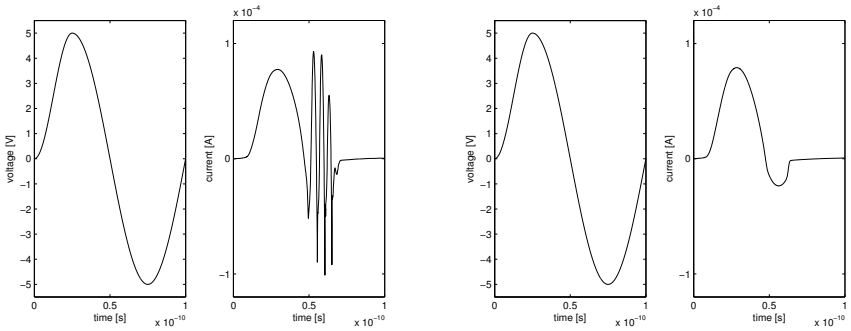

Fig. 5. Voltage and current through the diode for one bad case where the relative error is of order one (left), compared to the correct solution, where the full and GNAT-reduced solution is indistinguishable (right).

like DASPK could not be used. In the examples, we use the implicit Euler method and the trapezoidal rule as time integrators with equidistant time steps.

Because the residual function R depends on the time discretization scheme, the implementation is more complicated and complex, if adaptive time integration with order control is used. For variable order, we have to implement different residual functions.

The order of the time descretization scheme used for the GNAT (and other) reduced system should not be lower then the order of the time descretization scheme used for the full system to avoid performance loss due to smaller time steps. In the examples, we use therefore the same scheme for the full and reduced systems.

5.3 Assets and drawbacks of GNAT and POD-DEIM

In contrast to POD-DEIM, GNAT does not reduce the test spaces, so all equations are used to calculate the best approximation. This can lead to more accurate approximations.

In the case of multiple equations the residuals have to be scaled in order to consider all equations sufficiently in the residual. This is additional work but may offer the possibility to increase the influence of important equations.

The unscaled Jacobi-matrix used in the GN-iteration of the DD-equations is scaled very badly. The condition number is greater then $1e16$, which leads to numerical rank deficiency. Therefore, scaling is necessary to avoid unbalanced distribution of the degrees of freedom. Without such a proper scaling the result of the GNAT (T2) model in general is wrong.

To overcome this problem, we evaluate the functional R at the POD solution, and finally equilibrate the six equation blocks for this solution. A weighted L^2-norm is obtained in this way. Even after this scaling the Jacobi-matrix for the DD-equations is still badly scaled, but is sufficient to calculate the solution.

In the examples DEIM requires only as many indices as the number of basis functions, because the approximation is only done for the nonlinear part of the function. The linear part is approximated with POD. The GNAT (T3) method on the other hand needs in the example more then twice as many indices to calculate the basis functions for R and J_k to reach the accuracy of the (T2) method.

The GNAT (T3) model error may increase also for a low lack of information (LOI), see Figure 3 (upper left). This is due to the approximation of the equation ($g_\psi = \text{ grad } \psi$) in the GNAT (T3) model only at some selected points. The behavior of the (T3) model is improved and it turns out to be indistinguishable to the (T2) model even for very low LOI, if only this equation is not further reduced. This means that all the equations are used, as in the (T2) model. The different discretization of the potential and the gradient may be a problem for GNAT (T3). There may be other methods to deal with this problem more successfully.

6 Conclusions

We implemented POD-DEIM and GNAT for MOR of semiconductors in networks. It is one results of this research that the GN-iterations in this approach have to be well initialized, and the residual has to be scaled carefully in the case of MOR for multi-component PDE systems. In the investigated application it seems to be favorable to use POD-DEIM as MOR approach, since it delivers well approximating nonlinear reduced order models and also is very flexible and robust in implementation.

Acknowledgements The work reported in this paper was supported by the German Federal Ministry of Education and Research (BMBF), grant no. **05M10GUA** within the collaborative research project MoreSim4Nano. Responsibility for the contents of this publication rests with the authors.

References

1. Anile, A., Mascali, G., Romano, V.: Mathematical problems in semiconductor physics. Lectures given at the C. I. M. E. summer school, Cetraro, Italy, July 15–22, 1998. Lecture Notes in Mathematics. Berlin: Springer (2003)
2. Bodestedt, M., Tischendorf, C.: PDAE models of integrated circuits and index analysis. Math. Comput. Model. Dyn. Syst. 13:(1), 1–17 (2007)
3. Carlberg, K., Cortial, J., Amsallam, D., Zahr, M., Farhat, C.: The GNAT nonlinear model reduction method and its application to fluid dynamics problems, in AIAA 1969 (2012)
4. Carlberg, K., Farhat, C., and Bou-Mosleh, C., Efficient non-linear model reduction via a least-squares Petrov-Galerkin projection and compressive tensor approximations," International Journal for Numerical Methods in Engineering, Vol. 86, No. 2, pp. 155-181. (2011)
5. Gajewski, H.: On existence, uniqueness and asymptotic behavior of solutions of the basic equitions for carrier transport in semiconductors, ZAMM 65:2, 101-108 (1985)
6. Günther, M.: Partielle differential-algebraische Systeme in der numerischen Zeitbereichsanalyse elektrischer Schaltungen. VDI Fortschritts-Berichte, Reihe 20, Rechnerunterstützte Verfahren, Nr. 343 (2001)
7. Günther, M., Feldmann, U., ter Maten, J.: Modelling and discretization of circuit problems. Schilders, W. H. A. (ed.) et al., Handbook of numerical analysis. Vol XIII. Special volume: Numerical methods in electromagnetics. Amsterdam: Elsevier/North Holland. Handbook of Numerical Analysis 13, 523-629 (2005)
8. Hinze, M., Kunkel, M.: Discrete empirical interpolation in pod model order reduction of drift-diffusion equations in electrical networks. SCEE Proceedings 2010, Toulouse (2010)
9. Hinze, M., Kunkel, M.: Residual based sampling in POD model order reduction of drift-diffusion equations in parametrized electrical networks. ZAMM 92:91-104 (2011)
10. Hinze, M., Kunkel, M., Steinbrecher, A., Stykel, T.: Model order reduction of coupled circuit-device systems. Int. J. Numer. Model. 25:362-377 (2012)
11. Hinze, M., Matthes, U.: MoreSim4Nano TP6: Model Order Reduction of Electrical Networks with Semiconductors modelled by Quantum-Drift-Diffusion Models. Preprint Nr ????
12. Ho, C., Ruehli, A., Brennan, P.: The modified nodal approach to network analysis. IEEE Trans. Circuits Syst. 22, 504–509 (1975)
13. Selva Soto, M., Tischendorf, C.: Numerical analysis of DAEs from coupled circuit and semiconductor simulation. Appl. Numer. Math. 53:(2-4), 471–488 (2005)
14. Tischendorf, C.: Coupled Systems of Differential Algebraic and Partial Differential Equations in Circuit and Device Simulation. Habilitation thesis, Humboldt-University of Berlin (2003)